

Degradation of Dioxin-Like Compound, 3, 3', 4, 4' - Tetra Chlorobiphenyl, (PCB 77) Using Palladium-Copper Bimetallic Aerogels

Adelaide Baraza, Selline. A. Ooko, and Benard Omogo*

Department of Pure and Applied Chemistry, Masinde Muliro University of Science and Technology Kenya.

*To whom correspondence should be addressed

Corresponding Author: Adelaide Baraza

Abstract: Dioxin-like compounds such PCB-77 are highly toxic environmental persistent organic pollutants. Their environmental persistence nature is due to strong carbon-chlorine (C-Cl) bonds on their structure making them harmful to both humans and especially aquatic life. Due to this, their international production was banned by the Stockholm convention on POPs in 2001. However, poorly managed landfills and incinerators could still release them into our environment. One way of reducing their toxicity is by chemical degradation by an aid of a catalyst. This research was designed to explore the ability of palladium-copper (Pd-Cu) bimetallic aerogels as catalysts for degradation of PCB 77, a dioxin like compound which is classified as a carcinogen. Three ratios of Pd-Cu (1:1, 1:5, 1:10) were synthesized and confirmed using ICP-OES. The synthesized aerogels were used to degrade the PCB 77 for a total of 360 minutes and the products analysed using GC-MS. Results revealed that the co-planar PCB 77 had been degraded to a less toxic ortho-substituted PCB 47. Therefore, results from this study are of great benefit and contribution as one of the strategies towards minimizing the prevalence of chlorine based persistent organic pollutants.

Key words: Dioxine, Pd-Cu, Nanocatalyst, PCB47

Date of Submission: 13-11-2019

Date of Acceptance: 27-11-2019

I. Introduction

1.0 Introduction

The dioxin-like PCB 77 has a relatively higher toxicity equivalence factor (0.0001) compared to other tetrachlorobiphenyls [1, 2]. It binds on the same AhR protein receptor just like the dioxins [3]. PCB degradation is necessary even when the substances which are releasing the dioxin-like compound are no longer being used so that they do not pose a threat in the long run. This could be achieved by either changing the structural conformation of the pollutant or simply reducing it to less toxic level. In other words the term degradation as used here is not restricted to structural deformation but covers other forms of transformations including rearrangements of the chlorine atoms so long as the resulting products have reduced toxicity.

1.1 Nanoparticles

For the degradation, research has been directed towards the use of nanotechnology since nanoparticles are selective, stable, easily separable, energy efficient, atom economy and highly reactive due to large surface area leading to high productivity [4]. Among the nanomaterials, bimetallic nanoparticles catalysts have been proved to provide superior properties due to the presence of two metals. They exhibit greater surface area which increases the adsorption powers thus acting as more efficient catalysts when compared with the monometallic nanoparticles counterparts [5]. However, the challenge is how to produce bimetallic nanoparticles whose cost is low, having high activity, more durable and whose preparation is reproducible. To overcome this challenge, aerogels, a highly porous structure are prepared by gelling the preformed colloidal nanoparticle solutions then subjecting to controlled drying [6-8], have proved to be the best candidates. Some of the advantages of this material are that they do not necessarily need supports material for catalysis, have very low density which enables them to remain suspended in the solution and have high surface area which improves their catalytic performance and durability. In other words, they enhance the specific properties of nanoparticles to macro scale making them superior [8].

Preparation of aerogels involves two approaches [8]. The first approach also called the two step approach, leads to the formation of the sol; conversion of monomers into colloidal solution which acts as a precursor for the second stage in which an intertwined 3 dimensional network is formed. This gelation process leads to the formation of sol-gel also called hydrogel; a stable suspension of colloid solid particles in an aqueous

solution. This type of assembly is simple, economic and a cost effective procedure and ensures that the nanoparticles formed are of good quality with monodisperse distribution. Besides this, it also gives rise to nanoparticles with controlled morphology and size.

On the other hand, the one step approach, which involves the reduction and subsequent gelation of the nanoparticles produces particles with wide size distribution [8]. In the current study we undertook to prepare bimetallic aerogels using palladium and copper. Palladium has ability to adsorb large volumes of hydrogen on its lattice structure as well as in the interstitial sites. Synthesis of aerogels of Pd-Cu bimetallic was achieved through the reduction of noble metal precursors PdCl₂.2H₂O and CuCl₂.H₂O followed by addition of freshly prepared sodium borohydride solution; in this case the sodium borohydride used acted as both, the reducing agent as well as the stabilizer.

1.2 Dioxin and Dioxin like Degradation

Degradation is necessary in order to lower the level of contamination to a safe level. This could be achieved by either changing the structural conformation of the pollutant or simply reducing it to less toxic level. In other words the term degradation is not restricted to structural deformation but covers other forms of transformations including rearrangements so long as the resulting products has a reduced toxicity. Several remediation strategies [9] have been used to degrade these eco-toxic substances including; use of landfills, deep well dredging, capping, microbial reduction, phytoremediation rhizoremediation, use of supercritical water oxidation, electrochemical method, chemical reduction. The traditional methods like land filling and high temperature incineration though very effective requires very high temperature approximately 1000°C, some were disruptive, unachievable and in some cases transferred PCBs from one location /one form to other without necessarily getting rid of the toxins. Deep well dredging makes it hard to monitor the impact /damage by the wastes to the environment.

Microbial degradation approach uses fungi and bacteria to reduce PCBs. Payne and workmates achieved 56% reduction of Arochlor 1260 using microbial reduction [10]. The method though greener, PCB congeners require certain cultures or bacteria which at times are hard to grow in laboratory. The method requires long monitoring time and is very labour intensive. Phytoremediation was used however this also is limited to the availability of plants and with the global concern of the climate change, may not be sustainable or may result into more environmental challenge. It is a long term strategy which lacks biochemical pathway. Jing et al [10] notes that even though supercritical water oxidation was used to achieve 93% dechlorination of Decachlorobiphenyl by Fang and co-workers, it led to the production of Hydrochloric acid which eventually corroded the system. There was also accumulation from solid deposits that required constant removal resulting in an increase in maintenance costs [10].

Chemical reduction in which calcium in ethanol under atmospheric pressure was used to convert PCB into less toxic substances with 78% achievement in 24 hours at 150 °C has been used [11], the reaction requires sophisticated facilities to work. Volpe used Iron in the dehalogenation of a chlorinated triallate [12], Kim used Zinc to degrade chlorophenols with good results compared to iron [13]. Even though Long et al achieved 98% degradation of PCB contaminated soils at 600°C [14], Palladized iron nanoparticles were to achieve faster reduction of 2, 3, 4 Trichlorobiphenyl compared to unpalladized iron [15]. Others like Seteni et al achieved degradation of PCB 77 at ambient conditions however used an external source of nitrogen to keep the nanoparticles strictly under anaerobic conditions and a requirement of hydrogen source besides using PAA/PVDF membrane which increases the production costs. They too observed oxidation of the iron nanoparticles [16]. In all these methods high temperature and pressure are mandatory. Some demand for absolutely anaerobic conditions if degradation is to be realized.

According to Kim *et al*, a mechanism in which zero valent iron was used to dechlorinate PCDD congeners with four chlorine atoms in aqueous solution was found to be very slow making it unattainable within a practical time [13]. In yet another study, use of zerovalent iron is hampered due to surface passivation caused by the formation of poor conducting iron oxide and accumulation of intermediate products [17]. Therefore this study was designed to specifically explore the ability of palladium-copper (Pd-Cu) bimetallic aerogels for degradation of PCB 77 at ambient conditions.

II. Material And Methods

2.0 Reagents

All chemicals were procured from the respective companies through local distributors. The 3, 3', 4, 4'-tetrachlorobiphenyl (PCB 77) CAS No. 32596-13-3 was purchased from Sigma-Aldrich 100% pure and was used in our degradation experiments and as standards for the analysis of the chlorinated products. Acetone, n-hexane, dichloromethane, ethanol, and methanol were purchased from (Merck, Whitehouse Station, NJ; 99.9% pure, HPLC grade) and used in extracting and analysis of PCB 77 and its metabolites. Sodium borohydride (99.99%) and PdCl₂.2H₂O were obtained from Sigma-Aldrich. Ethanol (99.5%) was purchased from Acros

Organics. Hydrochloric acid (37.4%) and CuCl₂.H₂O were obtained from Fisher Scientific. All solutions were prepared using deoxygenated- deionized water obtained from the Pure and Applied sciences department of Masinde Muliro University of Science and Technology.

2.1 Metal Precursors Preparations

The precursor concentrations were maintained at 0.1mM. The preparation of the palladium precursor was achieved by dissolving 0.17733g of PdCl₂.2H₂O in 10 mL of 0.2M HCl in 100ml beaker followed by hand stirring using a glass rod. The H₂PdCl₄ formed was diluted using 10mL of de-ionized water and made up 50mL mark. Similarly, 0.17048g of CuCl₂.H₂O was added to 10mL of de-ionized water with continuous stirring before adjusting the volume to 50mL mark.

2.2 Synthesis of the Pd-Cu aerogels

The synthesis of PdCu aerogels was conducted using the procedure as given by with slight modification [8, 18,19]. Three ratio of PdCu aerogels namely 1:1, 1.5 and 1:10 were synthesized by varying the overall amount of the copper precursor while maintaining that for the palladium at room temperature. The two precursor solutions were mixed and stirred using an electron mixer for 5minutes. 125mL of freshly prepared sodium borohydride (NaBH₄) solution (prepared by dissolving 0.94575g in de-ionized water) was added followed by continuous stirring for 30 minutes. The standard total metal concentration in the reaction solution was maintained at 0.2 mM. The reaction solution was divided and transferred to 100ml vials to allow the nanoparticles to form. The final black colloidal solution was allowed to settle beakers at room temperature as the gelling process proceeded. After seven days, the formed hydrogels were gently separated from the supernatant by decanting the liquid out of the beaker. The obtained hydrogels were then transferred to the 10 ml vials and carefully washed five times after every 1hr with 10mL of fresh de -ionized water to remove any unreacted precursor solution. The final solution was gradually phase transferred from aqueous solution to acetone by sequentially replacing the top water with acetone until the whole solution was acetone. This overall handling of the hydrogels was conducted cautiously to prevent the gels from deforming [20]. The gels were first exchanged into acetone to remove the sticky hydroxyl/polar surfaces and finally into the low surface tension n-hexane to reduce on shrinkage.

2.3 Drying of the hydrogels

Once the hydrogels had been transferred into the n-hexane inside the 10ml glass vials without screwing the lid, the solvent was left to evaporate slowly undisturbed at room temperature and pressure.

2.4 Aerogels Characterization

The characterization of the aerogels was conducted as follows. Ultraviolet-visible (UV-Vis) spectrometer available in the department of Pure and Applied Chemistry, Masinde Muliro University of Science and Technology, was used to confirm alloying of the bimetallic nanocatalysts. For each ratio, 25mg of the aerogels were dissolved in 2mL distilled water and then used for analysis. Deionized water was used for background correction of all ultraviolet-visible spectra. The ultraviolet-visible spectrum was then recorded at regular time intervals. Samples were loaded into 10 mm path length quartz cuvettes for investigation [21] from 200nm to 800 nm. The crystalline structure of the bimetallic aerogels was determined using a Bruker D2 phaser XRD operated at a voltage of 30kV and a current of 1mA a capillary tubes for total acquisition time of 30 minutes using X-celerater Phillips expert diffractometer between $2\theta = 10^{\circ}$ and 100° with step of 0.03° using Cu-K α 1 monochromatic radiation whose wavelength = 1.54056 Å. The PdCu aerogel monoliths were crushed; drop casted on the glass sample holder using acetone to ensure that the samples are well pasted on the glass before being used. The average sizes and shapes of the particles were analyzed using Tecnai G2 20 TEM from FEI equipped with a laB6 cathode of an accelerating voltage of 200kV. TEM specimens were prepared by drop casting a dispersion of aerogels in acetone on carbon coated TEM grids (Kuhn et al, 2016). The resulting ratio of PdCu aerogels after synthesis was determined using Inductively Coupled Plasma-Optical Emission Spectroscopy (ICP-OES). The measurements were made using Perkin Elmer 2000DV ICP-OES instrument as described in the procedure in [22] and the ratio were compared to those of the original precursor ratios. X-ray diffraction spectroscopy (XRD), Transmission electron microscopy (TEM) and inductively coupled Plasma-optical emission spectroscopy were done at the Technical University of Dresden, Dresden, Germany.

2.5 Degradation experiments

2.5.1 Preparation of the external/stock standard

PCB77 the target congener solution was prepared by dissolving 0.01mg of PCB77 (CAS No. 32596-13-3) into 10ml acetone and analyzed using gas chromatography- mass spectrometer (GC-MS). The solution was stored below 4°C to avoid volatilization of the acetone.

2.5.2 Percentage Recovery from Extraction

Recovery was done to determine the effectiveness of the extraction process (equation 1).

$$\% \text{ Recovery} = \frac{\text{Amount recovered}}{\text{Amount expected}} \times 100 \quad (1)$$

2.5.3 Residual rate of PCB77 after 360 minutes

The residual PCB 77 calculated using equation 2, where C_t is the concentration of PCB77 at time t , C_o is the initial standard concentration. [23].

$$\text{Residual rate} = \frac{C_t}{C_o} \times 100 \quad (2)$$

Degradation Efficiency (DE) was calculated using equation 3[24].

$$DE = \frac{C_o - C_t}{C_o} \times 100 \quad (3)$$

2.5.4 Sample Preparation

The degradation experiments were performed through a modified liquid –liquid extraction method following the procedure described in [25]. Basically, 100ml of 40% ethanol-water co-solvent was measured and transferred to a 250ml clear volumetric flask and about 1g of PdCu (1:1) was added. This was then followed by spiking of 1000 μ L of 10ppm of PCB77 stock solution. The samples were then taken to an orbital shaker where the mixture was tumbled at a speed of 200 rpm to keep the nanocatalysts suspended for optimum mixing before centrifuging for 5 minutes. 10 mL of the sample aliquots were taken at predetermined times (60 minute intervals for 6 hours) and extracted into the DCM (HPLC grade/) by shaking on a touch mixer for 1 min. The aqueous and organic phases were separated by centrifuging at 6,000 rpm in a centrifuge for one and half minutes. The water free organic part was carefully separated out and was analyzed using gas chromatography-mass spectrometer (GC-MS). It is important to note that, all degradation experiments were performed at ambient conditions. This procedure was repeated for PdCu (1:5) and PdCu (1:10)

2.6 PCB Analysis

The quantification of PCB 77 was done using GC –MS (Agilent Technologies USA) Spectrophotometer GC-6890N equipped with a thermo scientific trace Gold GC capillary column (DB +5 Capillary 30 m x0.25mmx0.25 μ m) and connected to an Agilent 5973 Mass selective Detector(USA) found in the university of Nairobi. The Mass Spectrometer (MS) was operated in EI+ mode in the resolution of >5000 in full scan mode. Ultrapure Helium 99.999% was used as carrier gas at 1ml min⁻¹. Oven was maintained initially at 90° C for 1 min, the increased at 35 °C/min to 185° C, thereafter at 5 °C/min to 190°C with a hold time was 5 min at 10° C/min to 220 °C with a hold time of 5min, 25 °C to 250° withhold time 5 min and finally at 25° C/min to 320 °C.

III. Results and Discussions

3.1. Elemental Composition of PdCu Ratios.

ICP-OES technique was used to verify the elemental composition of the various ratios of Pd and Cu. This technique was selected due to its high sensitivity and ability to detect very low concentrations. The ratios from the ICP-OES were consistent with the theoretical values (table 1). The slight deviation could be attributed to the experimental error whereby fewer Pd⁰ particles formed during the reduction process as compared to Cu⁰ nanoparticles NaBH₄ reduced the divalent Pd²⁺ into their corresponding zerovalent Pd⁰ metal which then catalysed the reduction of Cu²⁺ to Cu⁰ before they were fused into the PdCu bimetallic hydrogels. This may explain why the amount of the palladium may be reduced.

Table 1. Comparison between the Actual ratios of the as prepared aerogels and the experimental ratios

Nanoparticles PdCu	Pd (mg/L)	Cu (mg/L)	PdCu (ICP-OES-ratios)
1:1	0.107	0.080	1 : 1.33
1:5	0.29	0.040	1 : 7.25
1:10	0.016	0.254	1 : 15.875

3.2 Analysis of bimetallic aerogels using UV-VIS spectroscopy

There were no absorbance maxima at approximately 400 nm and 600nm representing copper and palladium respectively [26]. Absence of absorbance maxima (figure 1) in the mentioned wavelengths points to the fact that alloying of palladium and copper had successfully taken place. This was a departure from findings by Blois et al where they suggested no alloying was seen for PdCu if Copper > 67% [27].

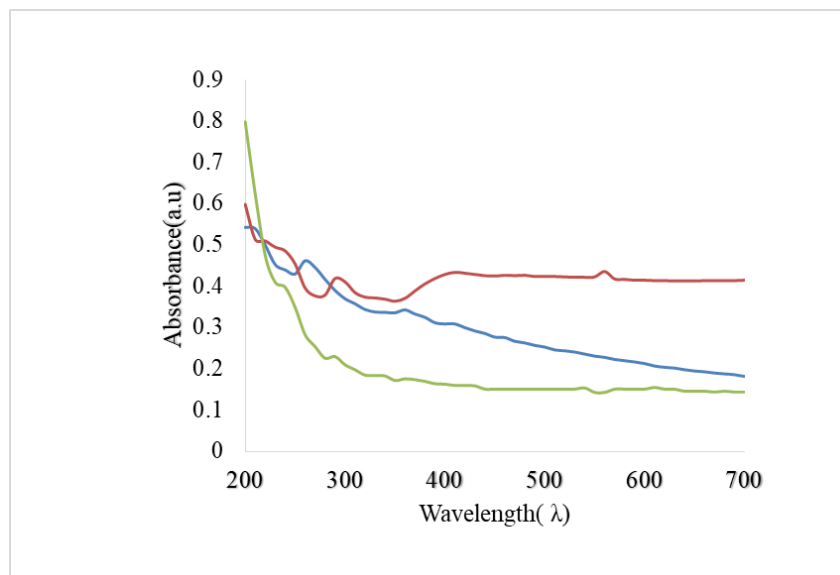


Figure 1: UV Vis Absorbance Spectra for PdCu1:1(red) PdCu1:5(purple) and PdCu1:10(blue) aerogels.

3.3 XRD analysis

The crystalline structure of the bimetallic aerogels was determined using X ray diffraction (XRD) spectrophotometer. The diffractograms displayed prominent peaks between $2\theta = 30^\circ$ to $2\theta = 50^\circ$. In figure 2, PdCu 1:10 had 3 strong peaks, PdCu 1:5 shows 2 strong peaks while PdCu1:1 had one broad peak; an indication of increased crystallinity with increase in the amount of copper. In other words the increase in the crystallinity of the bimetallic may be related to the increase in bimetallic ratio. The inter planar distances and lattice constants for the reflections were calculated through merging of two equations; the plane spacing equation (4) and the Bragg's equation (5) which are given below [28,29].

Inter planar spacing equation:

$$d_{hkl} = a^0 / \sqrt{h^2 + k^2 + l^2} \text{ (for cubic crystals)} \quad (4)$$

$$\text{Bragg's equation: } n\lambda = 2d\sin\theta \quad (5)$$

Where: d is the lattice /inter planar spacing,

a^0 is the inter atomic spacing calculated using

Bragg's law

$\sin \theta$ is the Bragg's angle for the particular reflection

h ,k, and l are the miller indices.

λ is wavelength of the electrons

n is an integer, the path difference between electrons scattered from adjacent crystal planes is $2d\sin\theta$.

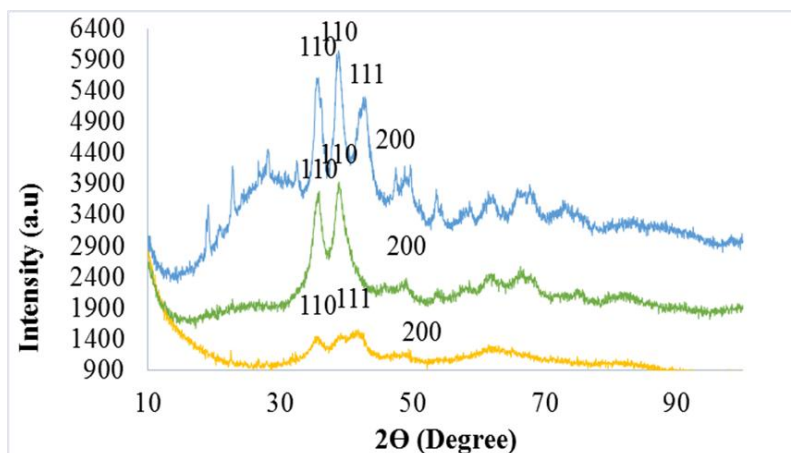


Figure 2: XRD spectra PdCu1:1(yellow), PdCu 1:5 (green), and PdCu1:10(Blue)

The reflections in bimetallic aerogel PdCu1:1 was located at 2θ values 35.8° and 40.7° . PdCu1:5 peaks appeared at 2θ values 35.7° and 38.7° while PdCu1:10 peaks appeared at 35.8° , 38.9° and 42.3° . The peaks that were assigned to their corresponding planes using miller constants calculated following Protocol by [30]. The distinct peak in PdCu 1:1 was assigned to the plane 110. Those in PdCu 1:5 were assigned to planes (110) and finally those in PdCu 1:10 were assigned to planes at (110,110,111). The first peak in a diffractogram represents the planes with the lowest Miller indices which also is an indication to the structure of the crystalline lattice [28]. All the three catalysts had a peaks assigned to the plane 110, an indication that they all had body centred cubic crystal structure (BCC). The presence of peak 111 may have been due to non-alloyed zero valent Pd⁰. The average lattice constants for the three bimetallic aerogels were PdCu 1:1 = $3.791 \pm 0.053115 \text{ \AA}$, PdCu1:5 = $3.771 \pm 0.053386 \text{ \AA}$ and PdCu 1:10 = $3.747 \pm 0.053742 \text{ \AA}$. The average lattice constants of the aerogels lie between that of FCC structure of pure palladium (3.882 \AA) and that for pure copper (3.585 \AA) which is an indication of alloy formation [29].

Generally, there is a decrease in the value of the lattice parameters from PdCu 1:1 to PdCu 1:10. The Size of the alloyed PdCu unit cell decreased with an increase in the amount of copper. Lattice constants decreased with increasing copper contents in the bimetallic due to the permeation of the small copper atom in the palladium lattice alloy [31]. The values of the lattice constants realized in this study were in agreement with those by [32]. The average inter-planar spacing for the three catalysts were, $2.421854 \pm 0.085586 \text{ nm}$, $2.407578 \pm 0.086094 \text{ nm}$ and $2.317557 \pm 0.089438 \text{ nm}$ for PdCu1:1, 1:5 and 1:10 respectively. The results were consistent with those obtained from another study which reported inter planar spacing of 2.7, 2.6 and 3.5 nm for PdCu with varying percentages of copper concentrations [22]. The lattice constants calculated using Bragg's equation were compared (table 2) to those calculated using both Nelson and Vergard's using equation 6 and 7 respectively.

$$F(\theta) = 1/2(\cos^2\theta/\sin\theta + (\cos^2\theta/\theta)) \quad (6)$$

$$a_{AB} = (1-x_B)a_A + x_B a \quad (7)$$

Table 2: Compares the lattice constants calculated from Vergard's law, Riley- Nelson and XRD.

Catalyst	Mole ratio of Pd from prepared amounts)	Lattice constants from Vergard's law	Lattice constants from Nelson- Riley Fn (Å)	Lattice constants from Bragg's law a* (Å)
1:1	0.50	3.80	3.95	3.79
1:5	0.83	3.70	3.85	3.77
1:10	0.91	3.60	3.72	3.75

Whereas the lattice constants calculated from the XRD results did not show significant deviations from one another they however deviated slightly from those of Bin Cai and Lindgren. The constants calculated using Riley- Nelson and Vergard's law were consistent with the literature by Lindgren [31,33].

3.4 TEM Analysis

Transmission electron microscopy (TEM) was used to determine the distribution in sizes of the particles as well as the morphology of the bimetallic aerogels. TEM was preferred due to its ability to elucidate detailed information on the size, shape and distribution of the formed aerogels unlike other techniques such as XPS that is mainly surface specific.

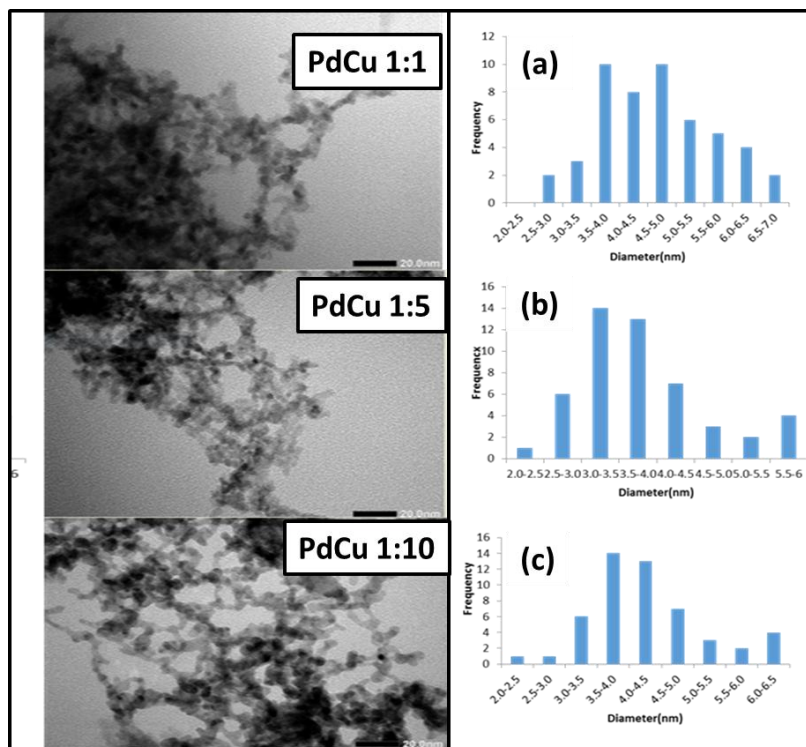


Figure 3. TEM images of PdCu1:1, PdCu 1:5 and PdCu 1:10 and respective histograms (a), (b) and (c).

Besides this, the TEM images clearly show the pores size distribution, an aspect that is very important while analysing aerogels for catalysis. The characterisation of the shapes of the particles of the as-synthesized PdCu aerogels was achieved using a FEI Tecnai F30 microscope operated at 200kV which is satisfactory to provide good resolution for the expected aerogels size. The TEM images obtained from the as-synthesized bimetallic aerogels are shown in figure 3 above with their corresponding histograms showing the size distributions. The analysis of TEM images to get an estimate of their average sizes and porosity was successfully achieved with the assistance of image J software and excel 2010. The TEM images were recorded at five different magnifications namely 25K, 50K, 100K, 200K and 500K. From the results, it was clearly visible that the as-synthesized aerogels were in nanoparticle range with sizes ranging between 3.840nm to 4.684nm.

As seen from the results, TEM images revealed a well assembled 3-D porous network of intertwined/chain-like structure with spherical shapes in all the three catalysts. The PdCu1:1 aerogel had the lowest percentage porosity while the PdCu1:10 aerogel had largest percentage porosity. Comparison between % porosity and size revealed that the percentage porosity reduced with increased crystal size. Porosity ranged from 49.122% - 55.739%. The bigger the size of the particle the lesser the size of the pores, the more porous a catalyst is the higher the number of the catalytic sites enabling faster catalytic ability. The % porosity approximately 50% was relatively good. The porosity could have been affected during the process of transferring of solvents which might have caused shrinkage of the aerogels. The representative histogram figure 3 drawn shows a unimodal size distribution of the aerogels, an indication that they were homogeneous. With higher porosity and smaller size PdCu1:10 was expected to be a better catalyst than the other two because crystal structure of a catalyst has greater bearing to its selectivity since the structure is a function of the molecular orientation in the catalyst [34].

3.5 GC MS Analysis.

3.5.1 Recovery.

Recovery was done to determine the effectiveness of the extraction process. After GC-MS measurements, the mean peak area of injected 1.4270mL of 10ppm PCB77 standard was 14290936 while that of the recovered 1.3426mL was 12176857 by volume. The recovery was 90.603% and thus good, since it was within the acceptable range for trace analysis which is between 80-120 % [23]. DCM was used for extraction due to its high extraction efficiency.

3.5.2 Identification of Metabolites

The products from the GC MS analysis were identified using the NIST library software together with RTECS. From which PCB 47 continued accumulating as the concentration of PCB 77 reduced.

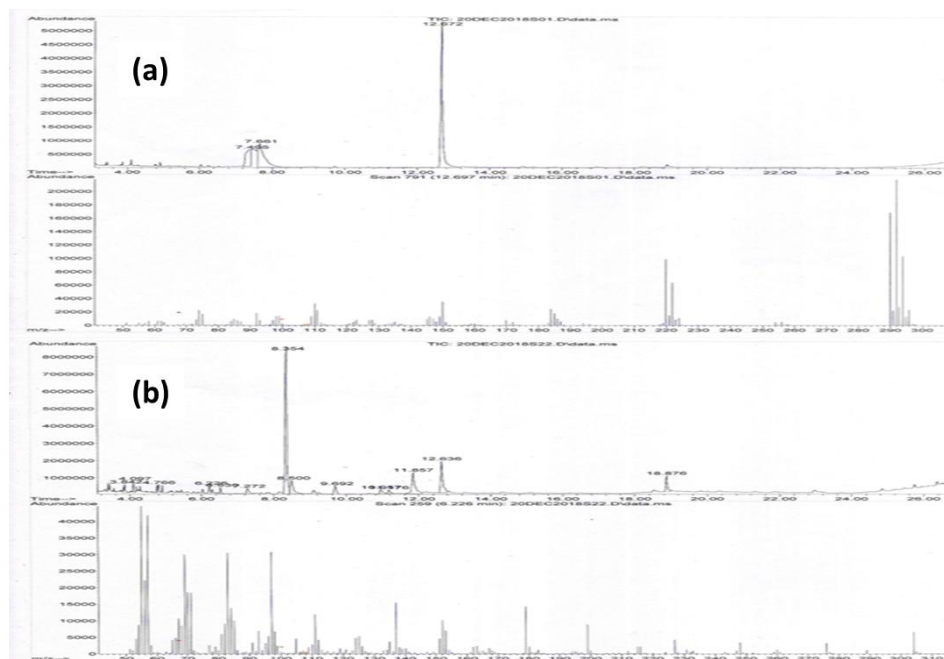


Figure 4. Chromatograms and Mass Spectra obtained from GC-MS both (a) PCB 77 and (b) PCB 47.

The accumulation of PCB 47 as the final product was indication that the congener was not further broken down. All the catalysts showed selectivity towards PCB 47, the selectivity being highest in the sample with PdCu 1:1. The chromatograms from the GC MS analysis are in figure 4. PCB 47 the daughter congener identified as the most dominant had retention time 8.379 minutes.

3.6 Degradation Kinetics

3.6.1 Graphical Determination of Order of Reaction

To find out whether the degradation followed the zero, first or second order reaction kinetics, we drew the graphs for concentration against time, natural logarithm of concentration against time and finally that of reciprocal of concentration against time for all the three samples.

3.6.2 Variation in Concentration of PCB 77 with Time

The degradation curves for PdCu1:1 and PdCu 1:5 had similar trend. The plots of concentration against time for all the three catalysts were not linear, ruling out the possibility of a zero order reaction figure 5(a). The highest drop in concentration was witnessed between 0 – 120 minutes. A graph showing natural logarithm of the concentration against time was plotted to further identify the reaction order figure 5b

Having calculated the analyte concentrations the values were fitted in the first order rate law, equation 8 below.

$$\ln [A]_t = -k t + \ln [A]_0 \quad (8)$$

$$1/[A]_t - 1/[A]_0 = k t \quad (9)$$

$$t_{1/2} = \ln 2/k = 0.693/k \quad (10)$$

Where: $[A]_t$ and $[A]_0$ represents the concentration of the PCB 77 at time t and $t=0$ and k is the slope at time t minutes.

3.6.3 Variation of natural logarithm of concentration with time

The results show that the graphs showing plot of natural logarithm against time (figure 5a) had linear fit after concentration of the samples were fitted into equation 9; PdCu 1:1 had an equation $y = -0.0029x + 16.274$ with a correlation coefficient $R^2 = 0.9687$, PdCu 1:5 had an equation $Y = -0.0042x + 16.225$ with a correlation coefficient $R^2 = 0.9844$ and while PdCu 1:10 had an equation $Y = -0.0041x + 16.24$ with a correlation coefficient of $R^2 = 0.9358$. All the plots had linear correlation coefficient above 0.9358 showing good linearity. All the three graphs in figure 5b were linear with negative slope these results fitted well in the first order rate law. The rate constants were 0.0029 ± 0.004 , 0.0042 ± 0.0006 and $0.0041 \pm 0.001 \text{ ng ul}^{-1} \text{ min}^{-1}$. Half-life of PCB77 degradation was determined using equation 10 and found to be $t_{1/2} = 238.966 \text{ (min}^{-1})$, $t_{1/2} = 165.500 \text{ (min}^{-1})$ and $t_{1/2} = 169.020 \text{ (min}^{-1})$ for PdCu (1:1), PdCu (1:5) and PdCu (1:10) respectively. These results suggest that this degradation process is dependent on the initial concentration of the PCB 77. This shows the reaction favoured first order reaction kinetics which agrees with results from the study by [24, 35].

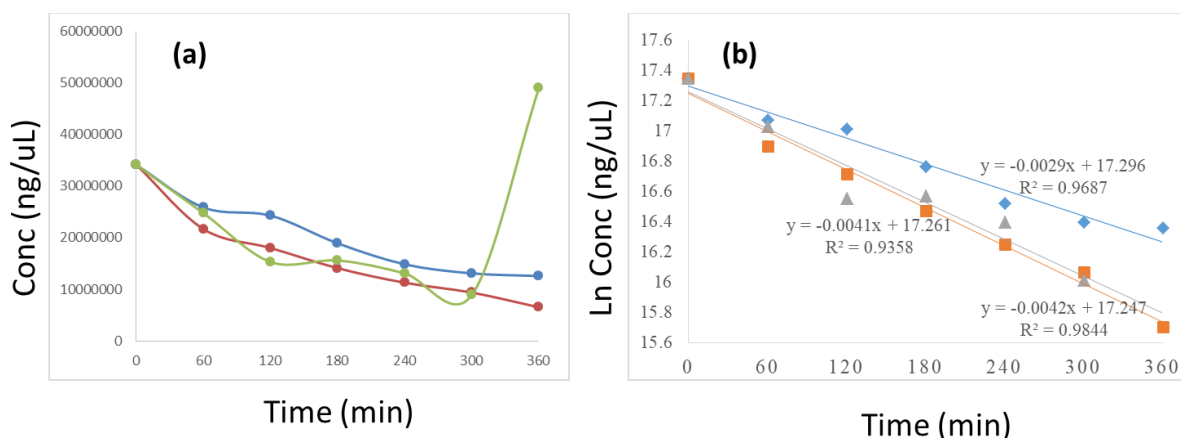


Figure 5. Variation of (a) concentration (b) natural logarithm against time

3.7 Residual rate of PCB 77/ Degradation efficiency after 360 minutes

The residual rates were 37.03% ± 0.4434 in (PdCu1:1), 19.33% ± 0.5530 (PdCu1:5) and 143.51% ± 0.3965 in (PdCu1:10). The concentration of PCB77 reduced up to 26.2799 in the first 300 minutes but quickly short up in the 360th minute (figure 6a). The degradation efficiency (figure 6b) was 62.97 % (PdCu1:1), 80.67% (Pd Cu 1:5) and -43.508% (PdCu 1:10). These results further show that PdCu1:5 was the best catalyst having been fully alloyed, TEM and XRD results had shown that PdCu 1:10 had the highest porosity, smallest size and a larger surface area, it was expected that it would give the best degradation results (having degraded much faster reaching 73.72%) than the rest in the first 300 minutes. But the increase in the amount of copper might have made it hard for the target congener to adsorb itself on the catalyst. These results deviated from those of Zhang et al and Cain et al who suggested the PdCu 1:1 was the most efficient catalyst [31,36].

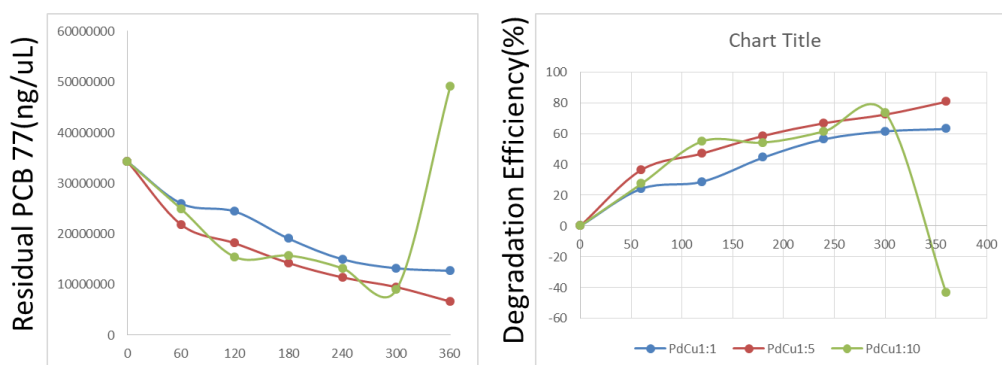


Figure 6. (a) Residual rate of PCB77 and (b) Degradation efficiency of PdCu1:1 (blue) PdCu1:5 (red) and PdCu1:10 (purple) up to 360 minutes

3.8 Degradation pathway/Rearrangement

The degradation pathway shown in figure 7 was actually a rearrangement which began with PCB77(3,3',4,4'-TeCB) → PCB80(3,3',5,5'-TeCB) → PCB78(3,3',4,5'-TeCB) → PCB72(2,3',5,5'-TeCB) → PCB70(2,3',4,5'-TeCB) and finally PCB47 (2,2',4,4'-TeCB). The chlorine atoms were not removed from the parent PCB77 congeners instead were rearranged from one position to another. This further suggests that the reaction progressed through electrophilic attack and thereby agrees with Pervova et al who proposed that when dechlorination progressed through electrophilic attack chlorine atoms are never removed [37]. The rearrangement begun with the transformation of chlorine atoms in the para position followed by those in the meta position. The ones in the ortho position were not transformed suggesting that the attack was on para > meta > ortho which is consistent with Liu *et al*, 2009 [38].

3.9 Mechanism of degradation

PCB 77 is an organic compound which consists four chlorine atoms which are shared by two benzene rings joined through a single bond. The chlorine atoms in position 4, 4' are para to the single connecting bond which is assigned position 1. Those in position 3, 3', are in the meta position. In PCB 77, C=C bond attached to the two chlorine atoms in each ring have a similar charge, since they are both partially positive. The chlorine atoms attached to them bearing a partially negative charge. There is a strong inductive effect due to the presence of chlorine substituents which deprives the biphenyl the rings of electron. Due to uneven electron density the C-Cl bond becomes polarised making it more prone to oxidative addition. As a result, the electron distribution is destabilised, creating partially positive and negative ions. The C-Cl ends with an overall partially negative charge making it susceptible to oxidative addition. The attack also depends on charge distribution on the ring.

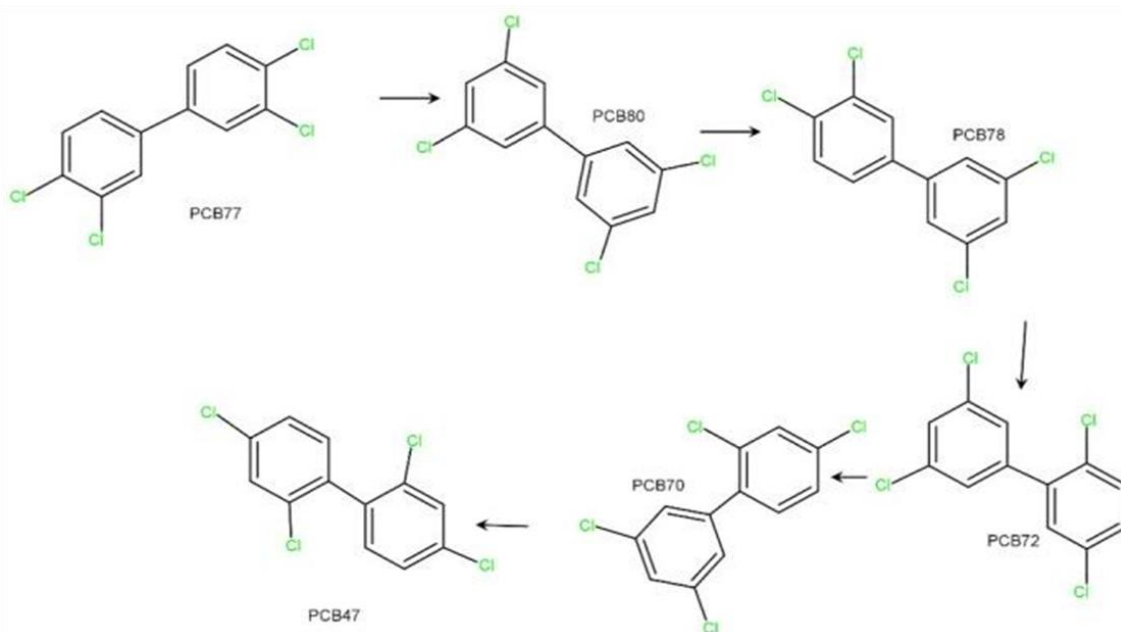


Figure 7. Schematic for the Rearrangement Pattern of PCB 77 when Exposed to the PdCu 1:1 Aerogel Catalysts.

Our findings suggest that the initial attack was on the carbocation on the meta position. It is however not confirmed how the Cl⁻ ion shifted to the ortho position, our most likely suggestion would be the already polarised C-Cl bond was easily attacked by the Pd-H which caused cleavage and subsequent expulsion of chlorine atom from the ring. As a result a carbocation was created in the already electron deficient ring. The chloride ion formed Cu-Cl (which is a strong bond) on the surface of the catalyst. Though as expected the Cl⁻ ion was supposed to bond with the H⁺ but because the Cu²⁺ ions which were in excess, preferentially combined with chloride forming Cu-Cl₂ in preference. Palladium with higher chemisorption capacity is able to reduce CuCl₂, releasing Cl⁻ back into the solution. Due to Pd ratio having been comparatively very low it was not able to release sufficient amount of dissociated hydrogen that would regenerate the Cu [39]. The Chloride ion was used to stabilise the ring by forming a bond with the adjacent charged carbon in the ortho position. The electrons in the pi bond between the already polarised benzene rings attack the electrophile (Pd -Cu surface) forming sigma bond, (one of the two carbons) with the electrophile. The remaining carbon acquires a positive charge thus destabilizing the aromaticity of the rings. The charge is further relocated to the other six carbon atoms and

alternates between the meta and para in to the location of the attack by the electrophile, forming a benzenonium intermediate. If the carbon in the meta position on both rings (to the location of the attack) is bonded to the released chloride ions, then 2,2',4,4', if it bonds with the carbon in meta and para position then 2,2',5,5' is formed. Other compounds formed were 2, 3'4, 5' depending on the location of the positively charged carbon. Liu et al also reported rearrangement of PCB77 during bioremediation using Poplar plants however mechanism is not known [38]. The fact that the degradation product PCB 47 could not be degraded further but instead continued accumulating further supports the fact that no chlorine atoms are removed from PCBs in an electrophilic reduction of PCBs [37].

IV. Conclusion

This study has demonstrated that PdCu aerogels are effective degradation agents of dioxin like compounds. Ironically the PdCu1:1 aerogel had the lowest percentage porosity while the PdCu1:10 aerogel had highest percentage porosity but the former was most effective in the degradation among all the three ratio used. The aerogels used here demonstrated a special kind of degradation known as rearrangement that does not reduce the molecular formula of the compounds but instead rearranges them to less toxic counterparts. For instance PCB 77 was hereby rearranged by PdCu to PCB 47, which is nontoxic congener.

Acknowledgement

We thank the Technical University of Dresden Germany especially Nikolai Gaponik and Dr. Nelli Weiss for their assistance with characterization of the aerogels. We also extend our gratitude to Mr. Osoro from University of Nairobi for providing us with facility to carry out GC-MS analysis.

References

- [1]. WHO/Dioxins and their health effect on human health (2016) www.WHO.int>.Mediacentre> factsheets.
- [2]. Stockholm Convention on Persistent Organic Pollutants (POPs), (2002) Geneva, Secretariat of the Stockholm Convention (<http://chm.pops.int>)
- [3]. Rahumann.M.S.M.M.Pistone L., Tririfiro F.and Miertus S*(2000) Destruction technologies for polychlorinated biphenyls (PCBs) ICS-UNIDO 55pages. Aerogels Without pressure <https://www.aerogel.org>
- [4]. Liu, J., Qin, G., Raveendran, P., Ikushima, Y., (2006) Facile Green Synthesis, Characterization, and Catalytic Function of β -D-Glucose-Stabilized Au Nanocrystals. *Chem. Eur. J.* **12**, 2131–2138.
- [5]. Sharma,G.Kumar,A.Sharma,S.,Naushad,M.,Dwivedi,R.P.,ALothman,Z.A.,Mola,G.T.,(2017)Novel development of nanoparticles to bimetallic nanoparticles and their composites. *A Journal of King Usaid. A review* .www.science direct.com.
- [6]. Toshima,N.,Tokonami,S., Morita,N.,Tarakasi,K.,(2010)Novel synthesis ,structure and oxidation catalysis of Ag/Au bimetallic nanoparticles. *Journal of physical chemistry.* **114**, 10336-10341.
- [7]. Liu,W.,Herman,A.K.,Gaponik,N. and Eychmuller,A.,(2017)Mordern Inorganic Aerogels *Agewandte Chemie International Edition*.DOI:10.1002/Anie.201611552
- [8]. Kuhn.L.Herman.AK.,Rukowski.B.,Oeszaslam.M.,Nachttegaal.M.,Klose.M.,Giebeler.L.,Gaponik.N.,Eckert.J.,Schimddt.T.J.,Cryska.F.A.,Eychmuller.A.,(2016) Alloying behaviour of self-assembled Noble Metal nanoparticles/Chemistry –A European Journal. **22**,13446-13450.
- [9]. Jing, R., Fusi, S., and Kjellerup, B.V. (2018) Remediation of PCBs in contaminated soils and sediment; state of knowledge and perspective. *Frontiers in env.Sci.* **6**:79.doi:10.3389/fenvs.2018.00079.
- [10]. Payne,R.B.,May.H.D.,and Sowers,K.R.(2011)Enhanced reductive dechlorination of polychlorinated biphenyl impacted sediment by bioaugmentation with dehalorespiring bacterium. *Environmental Science Technology* **45**,8772-8779.doi.10.1021/es201553c
- [11]. Mitoma,Y.,Miyatab,H.,Egashiraa,N.,Simion,A.M.,Kakedaa,M.,and Simionc ,C.,(2011)Mechanochemical degradation of chlorinated contaminants in Fly –ash with a calcium –based degradation reagent. *Chemosphere* **83**, 1326-1330
- [12]. Volpe,A., Lopez, A., Mascolo, G., and Detomaso, A., (2004) “Chlorinated herbicide (triallate) dehalogenation by iron powder”, *Chemosphere.* **57**, 579-586.
- [13]. Kim, Y.H.and Caraway, E. (2003) Dechlorination of chlorinated Phenols by zerovalent zinc. *Environmental Technology* **24**(12) 1455-1463.
- [14]. Long,Y.Y.,Zhang,C.,Du,Y.,Tao,X.Q.,and Shen,D.S.(2014)Enhanced reductive dechlorination of polychlorinated biphenyl-contaminated soil by in vessel anaerobic composting with zerovalent iron. *Environmental Science Pollution Resources.* **21**, 4783-4792. doi: 10.1007/s11356-013-2420-4
- [15]. Kim, J.H., Paul, G., Tratnyek, P.C., and Chang, Y.S. (2008) Rapid dechlorination of Polychlorinated dibenzo-p-dioxin by bimetallic and nanosized zerovalent iron. *Environmental science technology.* **42**, 4106-4112
- [16]. Zhuang, Y.,Ahn,S.,Seyfferth,A.L.,Masue-Slowey,Y.,Fendorf,S.,and Luthy.R.G.,(2011) Dehalogenation of polybrominated biphenyl by bimetallic impregnated, and nanoscale zerovalent iron. *Environmental science Technology.* **45**,4896-4903.doi:10.1021/es104312h
- [17]. Seteni,B.,Ngila,J.C.,Sikwwivhilu,K.,Moutloali,R.M.,(2013).Dechlorination of 3,3',4,4'tetrachlorobiphenyl(PCB77) in water, by nickel/iron nanoparticles immobilized on Lysine/PAA/PVDF membrane. *Journal Physical chemistry.* *Earth* **66**, 60-67.
- [18]. Gunawardana, B., Singhal, N., Swedlund, P. (2012) Dechlorination of Pentachlorophenol by zerovalent iron and bimetallic effect of surface characteristics and bimetallic preparation procedures. *Proceedings of annual international conference on soils, sediments, water and energy.* **17** (8)<http://scholarworks.umass.edu/soilproceedings/vol17/Issue18>
- [19]. Liu,W.,Rodriguez,P.,Borchardt,L.,Foelske,A.,Yuan,J.,HermannA.K.,Geiger,D.,Zheng,Z.,Kaskel,S.,Gaponik,N.,Kotz,R.,Schmidt,J.T. Eychmuller.A.,(2013)Bimetallic Aerogels:High performance electrocatalysts for the oxygen reduction reaction *Angewandte Chemie International Editio* **52**(37).
- [20]. Aerogels Without pressure and <https://www.aerogel.org>
- [21]. Arunachalan, K.D., Annamalai, S.K., Hari, S. (2013). One step synthesis and characterization of leaf –mediated biocompatible silver and gold nanoparticles from memecylon umbellactum. *International Journal of Nano medicine* **8**.1307-1315.

- [22]. Shiyao, S., Petkov, V., Praskal, B., Wu, J., Joseph, P., Skeete, Z., Kim, E., Molt, D., Malis, O., Luo, J., and Zhong, C. (2015) Catalytic activity of bimetallic catalysts highly sensitive to the atomic composition and phase structure at nanoscale. *Nanoscale*, **7**, 18936
- [23]. Mohmoud, A. A. and Azees, A., (2017) Study of PCB in soil sample from Al-Ahdab oil field in Waset region. *Toxins review* **36** (2)
- [24]. Wang, Y., Si, X., and Si, Y., (2015) Dechlorination of 3,3',4,4' Tetrachlorobiphenyl in aqueous solution by hybrid Fe⁰/Fe₃O₄ nanoparticle system. *Journal of Experimental nanoscience*, **10**, 1166-1179
- [25]. Agarwal, S., Al-Abed, S. R. and Dionysiou, D.D. (2007); Enhanced corrosion-based Pd/Mg bimetallic systems for dechlorination of PCBs. *Environmental science & technology* **41**, 3722-3727.
- [26]. Ullah, I., Khan, K., Sohail, M., Ulla, K. Ulla, A. and Shaleen, S., (2017) Synthesis Structural characterization and Catalytic application of Citrate stabilised monometallic and bimetallic palladium @ Copper nanoparticles in microbial anti activities. **12**, 8735-8747.
- [27]. Blosi, M., Orтели, S., Costa, A.L., Dondi, M., Lolli, A., Andreoli, S., Benito, P., and Albonetti, S., (2016) Bimetallic Nanoparticles as efficient Catalysts: Facile and Green microwave synthesis. *Materials* **9**, 550
- [28]. Scott A speakman PhD. speakman@mit.edu. <http://prism.mit.edu/x-ray>
- [29]. Cullity, B.D. and Stock, S.R., (2001) Elements of X ray diffraction Second Edition
- [30]. Lufaso, M., (2013) Physical methods for characterizing solids. <http://www.unf.edu>.
- [31]. Cai, F., Yang, L., Shan, S., Mott, D., Chen, B. H., Luo, J., and Zhong, C-J., (2016) Preparation of PdCu alloy nanocatalysts for nitrate hydrogenation and carbon monoxide oxidation. *catalysts* **7**, 96
- [32]. Douk, A. S.; Majid F.; Damanigo, F.; Moghiddan, A. A.; Saravani, H. and Noroozifar, M. (2018) *Royal society of chemistry* **8**, 23539-23545
- [33]. Lindgren, C.M., (2014) Properties and applications of PdCu membranes for hydrogen separation. [http://www/pdf/semantic Scholar.org](http://www.pdf/semantic Scholar.org)
- [34]. Mukundan, V., Yin, J., Joseph, P., Luo, J., (2014) Nanoalloying and phase transformation during thermal treatment of physical Mixtures of Pd and Cu nanoparticles. *Science and Technology of Advanced Materials*. **15**(2); 025002
- [35]. Xin, L., Qui, Y., Li, W., Li, Y., Janik, J. M., Guo, F., Liu, Q and Ren, Y (2018) Understanding the role of PdCu nanoalloys for enhanced hydrogen oxidation reaction. *Advanced solid state and electrochemical science technology* MA2018-01 17
- [36]. Zhang, Z., Yang, N., Chen, B., Huang, Y., Chen, J., Sindoro, M., Wang, A., Cgeng, H., Fan, Z., Liu, X., Li, B., Zhong, Y., Gu, L. and Zhang, H. (2017). Synthesis of ultra-thin PdCu alloy Nano sheets Used as a Highly Efficient electro catalyst for formic Acid Oxidation *Advanced materials* **29**(29):1700769, 2017.
- [37]. Pervova, M.G., Platnikova, K.A., Mekhaev, A. V., Pestov, A. V., Saloutin, V. I., Chupakhin, O., (2016) Mass spectroscopic study of Bromination of Technical mixtures of PCB. *Springer* **466**, (2)29-34
- [38]. Liu, T. Hu, D., Hang, G. and Schooner J (2009) In vivo biotransformation of 3, 3', 4, 4' Tetrachlorobiphenyl by whole plants – poplars and switch grass. *Environmental Science Technology*. **20**, 7503-7509.
- [39]. Beteley, T. M. (2011) Hydrodechlorination of Chlorinated Organic wastes over Palladium Supported Mixed Oxide catalysts. DL:T.1347-2011

IOSR Journal of Applied Chemistry (IOSR-JAC) is UGC approved Journal with SI. No. 4031, Journal no. 44190.

Adelaide Baraza. "Degradation of Dioxin-Like Compound, 3, 3', 4, 4' - Tetra Chlorobiphenyl, (PCB 77) Using Palladium-Copper Bimetallic Aerogels." *IOSR Journal of Applied Chemistry (IOSR-JAC)* **12.11** (2019): 06-17.